LETTER

Surface-Step-Terrace-Induced Anomalous Transport Properties in Highly Epitaxial $La_{0.67}Ca_{0.33}MnO_3$ Thin Films

Hongliang Lu,[†] Chendong Zhang,[†] Haiming Guo,[†] Hongjun Gao,*[,†] Ming Liu,[‡,§] Jian Liu,[†] Gregery Collins,[†] and Chonglin Chen*[,†]

Institute of Physics, Chinese Academy of Sciences, Beijing 100190, P. R. China, Department of Physics and Astronomy, University of Texas at San Antonio, San Antonio, Texas 78249, and Department of Physics, Dalian University of Technology, Dalian 116024, P. R. China

ABSTRACT $La_{0.67}Ca_{0.33}MnO_3$ thin films were epitaxially grown on miscut MgO(001) substrates by pulsed laser ablation. Electrical transport properties were studied by using an ultra high vacuum, four-probe STM system at different temperatures. Anomalous resistivity behavior and metal−insulator transition temperatures were found, both of which are highly dependent upon the miscut angle (1, 3, and 5°). These phenomena are attributed to the difference in residual strain that results from the difference in terrace widths of the vicinal surfaces.

KEYWORDS: epitaxial thin film • miscut • mangnite • strain • metal−insulator transition

Strain is a nontrivial factor affecting the physical properties of epitaxial thin films. It can significantly alter their electrical conductivity, change the phase transition temperature, and affect other properties. For instance, dramatic changes in the Curie temperature have been observed in the highly epitaxial ferroelectric thin films (1); and strong effects on the phase-transition temperatures, magnetic properties, and electrical conductivity in the highly epitaxial Manganite thin films were induced by lattice mismatches between the film and the substrate (2−4). On the other hand, Chen et al. suggested that various antiphase domain boundary structures could be formed in highly epitaxial ferroelectric thin films by altering the dielectric tenability (5, 6). Microstructure studies by Jiang et al. further demonstrated that the microstructure of $Ba_{0.6}Sr_{0.4}TiO_3$ thin films can be strongly influenced by steps, terraces, and kinks of substrates by forming equally spaced misfit dislocations at the interface, with physical properties of the film accommodating their microstructures (7). Furthermore, it has been found that the physical properties are dependent not only on the strain generated from the lattice misfit between the film and substrate but also on the detailed surface-step dimensions. Chen et al. have systematically investigated the effects of the dimension of substrate surface-step terraces on the epitaxial nature and the physical properties (7−9). Recently, a model of local strain induced by surface-step-terrace dimensions was established to understand various physical phenomena in highly epitaxial oxide thin films. However, only limited data are available for understanding and examining the model.

To verify the effects of local strain on the physical properties of highly epitaxial oxide thin films, characterizing the electrical transport properties is one of the most practical techniques. Recently, we have systematically studied the effects of various surface step terraces on the physical properties of the highly epitaxial $La_{0.67}Ca_{0.33}MnO_3$ (LCMO) thin films. In this letter, we report electrical transport phenomena in highly epitaxial $La_{0.67}Ca_{0.33}MnO_3$ (LCMO) thin films on MgO (001) substrates with different miscut angles. We will show that the electrical resistivity and metal−insulator transition temperature (T_{M-I}) of the as-grown LCMO thin films are greatly modulated by changing the dimensions of the substrate terraces.

The $La_{0.67}Ca_{0.33}MnO_3$ thin films were grown on various (001) MgO vicinal surfaces by using pulsed laser deposition. Three types of miscut MgO substrates (1, 3, and 5°) along the ⟨100⟩ direction were adopted for studying the residual strain effect, respectively. The thickness of LCMO films is about 250−300 nm. The epitaxial quality and crystallinity of the LCMO films on various miscut MgO surfaces were examined by traditional X-ray diffraction (XRD) technique. Figure 1a is the typical X-ray diffraction pattern achieved from the 1° miscut sample. Both 3° and 5° miscut samples have similar spectra. The sharp {001} diffraction peaks and the small values of the rocking curve measurement results (all smaller than 0.2°) suggest that the as-grown films have good single-crystal quality and excellent epitaxial nature.

The resistivity of LCMO thin films were characterized in an Omicron ultrahigh vacuum (UHV) four-probe scanning tunneling microscopy (4P-STM) system using a Keithley

* Corresponding author. E-mail: hjgao@iphy.ac.cn (H.G.); cl.chen@utsa.edu (C.C.). Telephone: +86-10-82648035 (H.G.); (210) 458-6427 (C.C.). Fax: 86-10-62556598 (H.G.); 210-458-4919 (C.C.).

Received for review June 22, 2010 and accepted August 26, 2010

[†] Chinese Academy of Sciences.

[‡] University of Texas at San Antonio.

[§] Dalian University of Technology.

DOI: 10.1021/am100542n

Published on Web 08/31/2010

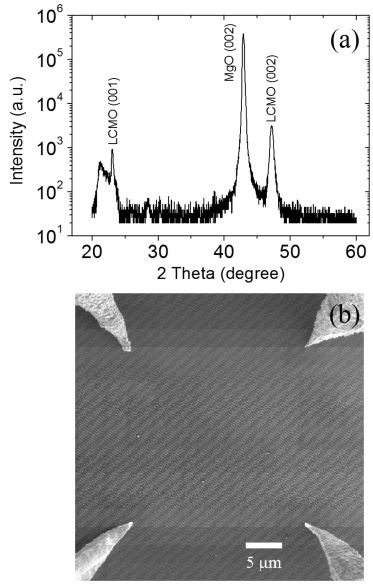

FIGURE 1. (a) Typical X-ray diffraction pattern of the LCMO thin film grown on a vicinal MgO surface. (b) SEM image showing the four gold tips in contact with LCMO surface.

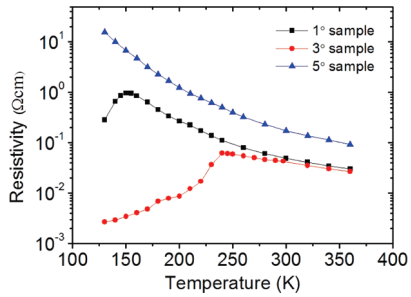

FIGURE 2. Temperature dependence of electrical resistivity of LCMO thin films on three vicinal MgO substrate surfaces with the miscut angles of 1°, 3° and 5°. The transition temperatures (T_{M-I}) are 153 and 238 K for the 1 and 3° samples, respectively. No transition was found for the 5° sample, on which the film is always insulating.

4200 apparatus and an in situ scanning electron microscope (10, 11). The square four-terminal method was used for measuring the resistance of thin films (12, 13). All four electrodes were gold tips, fabricated by a standard chemical etching technique, to ensure good electrical contact. Each tip can be independently operated in our system. Figure 1b is a typical SEM image of the four gold tips in contact with the sample surface. The contact separation spacing s is about 25 μm in this experiment. The scale of thin film is several mm. Four-terminal method requires that the film thickness d be extremely thin and the film size l is infinitely large, i.e., $d \ll s \ll l$, therefore such an experimental setup is considered good enough for the measurement requirements. The sample temperature is controlled by liquid nitrogen cooling and electrical heating in the range from 130 to 360 K. See the Supporting Information for experimental details.

Figure 2 shows the measured resistivity−temperature curves (from 130 to 360 K) of three different LCMO thin films. The resistivity is distinctly different among the three samples. At high temperature, the resistivities of the 1 and 3° samples are on the same order, whereas that of 5° sample is about 1 order of magnitude larger. The resistivity

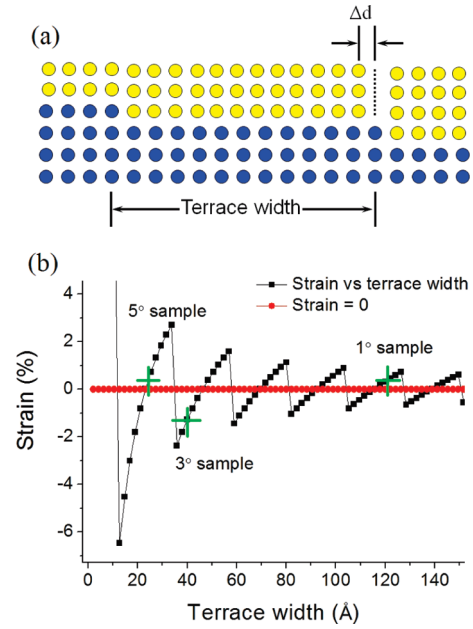

FIGURE 3. (a) Schematic of the atomic structures of the LCMO thin film on the MgO(001) substrate consisting of steps and terraces. If lattice constants in bulk materials and substrate terrace width (D) are known, the residual space (Δd) in film can be estimated. (b) Calculated surface-step-terrace induced strain of LCMO thin film vs MgO(001) substrate terrace width. The strain is defined as $(a_f' - a_f)/a_f$. The green crosses indicate corresponding strain in three samples with the miscut angles of 1, 3, and 5°.

difference in the three samples becomes enlarged at low temperature. Clearly, a metal−insulator transition can be seen in both 1 and 3° samples in the experimental temperature range (14). It should be noted that the metal−insulator transition temperatures (T_{M-I}) are markedly different in these two samples, 153 and 238 K for 1 and 3° samples, respectively. Furthermore there is no transition in the film grown on the 5° miscut substrate, and the film has a typical insulating behavior.

To understand the nature of these interesting physical phenomena, we systematically investigated microstructures and local strain of thin films on various vicinal MgO surfaces. As seen in Figure 3a, the simplified atomic structure of the LCMO thin film and MgO(001) substrate consisting of steps and terraces is schematically illustrated. If the atoms' positions in the substrate are fixed, the atomic spacing in the film must be tuned to fit the terrace width, which will generate a particular local strain. Because the lattice constants of the film and substrate differ, a residual space (Δd) must be generated in the terrace of the substrate, as shown in Figure 3a

$$\Delta d = N_s a_s - N_f a_f = D - N_f a_f \quad (1)$$

where D is the terrace width on the substrate, a_s and a_f are lattice constants of the substrate and film in bulk materials, respectively, and N_s is the number of substrate atoms on a terrace that can match the maximum number of film atoms N_f on one terrace to ensure a positive Δd value.

In most cases, the value of Δd is not equal to zero. Therefore, the atoms in the LCMO film will rearrange to

Table 1. Averaged Substrate Terrace Width, Surface-Step-Terrace-Induced Strain, And Measured Metal−Insulator Transition Temperature (T_{M-I}) for LCMO Thin Films on 1, 3, and 5° Miscut MgO(001) Substrates, Compared with Films on Smooth MgO(001) Substrate and Bulk LCMO Materials

specimen	terrace width (Å) (calcd)	surface-step-terrace-induced strain (%) (calcd)	T_{M-I} (K) (exp)
bulk	no	0	250 (ref14)
0°	∞	0	221 (ref16)
1°	120.65	0.36	153
3°	40.18	−1.24	238
5°	24.07	0.33	<130

reduce the residual space Δd. Thus, the resultant atomic spacing in the film (a_f') will become larger or smaller than the bulk value a_f. If Δd is much less than a_f, the residual space will be averaged by all atoms in film on the terrace and atomic spacing in the film will be elongated ($a_f' > a_f$)

$$a_f' = a_f + \frac{\Delta d}{N_f a_f} \tag{2}$$

Otherwise, if Δd is larger than a value, assumed to be $a_f/2$, a new row of atoms must be inserted into the residual space and thus the atomic spacing in the film is compressed ($a_f' < a_f$).

$$a_f' = a_f + \frac{\Delta d - a_f}{(N_f + 1)a_f} \tag{3}$$

Thus, the real atomic spacing in the film a_f' and consequently the strain fluctuate with variation of the terrace width on the vicinal MgO substrate. We define this strain as surface-step-terrace-induced strain $= (a_f' - a_f)/a_f$. To understand the effects of this strain on the transport behavior, we assume that there are only monatomic steps on the substrate, and the surface has a uniform density of steps so that only the average terrace width is considered. The bulk lattice constants of MgO, 4.212 Å (8), and $La_{0.67}Ca_{0.33}MnO_3$, 3.86 Å (15), are used in strain calculation and the result is shown in Figure 3b and Table 1. This strain is a main part of the total strain in the LCMO thin films, and hence is of great importance for their physical properties.

In 1° miscut sample the average substrate terrace width is 120.65 Å and the corresponding surface-step-terrace induced strain in LCMO film is 0.36%, tensile, as shown in Figure 3b and Table 1. Considering the tensile strain in LCMO film near film substrate interface, we believe tensile strain in the 1° miscut surface is greater than that in 0° surface. It has been demonstrated that the tensile strain can significantly decrease the T_{M-I} in Manganite epitaxial thin films (3, 4). The Curie temperature (T_C) of $La_{0.67}Ca_{0.33}MnO_3$ film on MgO (001) substrate with no miscut surface is 221 K (16), and T_{M-I} is considered to be approximate to T_C. Thus, the fact that the T_{M-I} value of 153 K in the 1° sample is much lower than the traditional value of 221 K should be carefully reviewed by considering the influence of the miscut vicinal surfaces.

Similarly, on the 3° miscut surface, the substrate terrace is 40.18 Å on average, and the corresponding surface-step-terrace induced strain is −1.24%. This compressive strain can mitigate the inherent tensile strain in the film to a certain degree, which suggests less tensile strain. It is interesting that the transition temperature value T_{M-I} is found to be 238 K, which is slightly higher than the value of 221 K (16) on the no-miscut surface and closer to that of bulk material, 250 K (14).

The resistivity behavior of the as-grown film on 5° miscut surface differ greatly from those on 1 and 3° miscut surfaces. It should be noticed that the average terrace width in the 5° miscut substrate is 24.07 Å, which means $N_f - N_s = 1$. Because $N_f - N_s$ is an odd number, an antiphase domain boundary must be formed at the surface step edge (8). Ions in the film at both sides of the antiphase domain boundary are charged in the same sign, so high strain must exist in this region. This high-strain region is very likely to change the structure of the MnO_6 octahedron locally and distort the Mn−O−Mn bond angle, which could lead to a significant increase of resistivity and alter the M−I transition temperature (17). A. Biswas et al. demonstrated that a charge ordering (CO) state appears in a high-strain region near the island edge and results in the insulating behavior of the film (18). Therefore, in the 5° miscut surface, the charge ordering state must form because of the existence of the antiphase domain boundary. On the other hand, in the 5° sample, the surface-step-terrace-induced strain is 0.33%, as indicated in Figure 3b and Table 1. The large tensile strain and formation of CO states in 5° sample both result in the decreasing of T_{M-I} and insulating transport behavior. In general, the antiphase boundary plays a key role in tuning the transport properties of the 5° sample.

It should be noted that it is possible to detect the strain effects on transport properties in films with thickness of 250−300 nm, as shown in (17), because the electrode separation is greatly larger than the film thickness and the current can penetrate into the whole thin film in four-terminal method (19).

In summary, the temperature-dependent resistivity of highly epitaxial $La_{0.67}Ca_{0.33}MnO_3$ films on various miscut MgO(001) substrates was systematically studied by using ultrahigh vacuum four probe STM system. The resistivity and metal−insulator transition temperatures were found to be highly dependent upon the miscut angles of 1, 3, and 5°, which can be attributed to the difference in residual strain that results from the difference in terrace widths of the vicinal surfaces. Together, the residual strain in the films and the effects of the antiphase boundary in tuning the properties of a film indicate a new approach for preparing functional thin film devices in nanoscale.

Acknowledgment. The authors gratefully acknowledge financial support from the Natural Science Foundation of China (NSFC, Grant 60976089), and the "863" (2008AA03Z309) and

"973" (2007CB936802) national projects of China. It is partially supported by the National Science Foundation under NSF-NIRT-0709293, the Texas ARP Program under 003656-0103-2007, and the State of Texas through the Texas Center for Superconductivity at the University of Houston.

Supporting Information Available: Experimental details for thin film growth, surface preparation, and electrical transport measurement, and detailed schematic illustration for microstructure of LCMO thin films in 1, 3, and 5° samples (PDF). This material is available free of charge via the Internet at http://pubs.acs.org.

REFERENCES AND NOTES

(1) Yanase, N.; Abe, K.; Fukushima, N.; Kawakuba, T. *Jpn. J. Appl. Phys.* **1999**, *38*, 5305–5308.
(2) Chen, X. J.; Soltan, S.; Zhang, H.; Habermeier, H.-U. *Phys. Rev. B* **2002**, *65*, 174402.
(3) Xiong, Y. M.; Wang, G. Y.; Luo, X. G.; Wang, C. H.; Chen, X. H.; Chen, X.; Chen, C. L. *J. Appl. Phys.* **2005**, *97*, 083909.
(4) Gillaspie, D.; Ma, J. X.; Zhai, H. Y.; Ward, T. Z.; Christen, H. M.; Plummer, E. W.; Shen, J. *J. Appl. Phys.* **2006**, *99*, 08S901.
(5) Liu, S. W.; Lin, Y.; Weaver, J.; Donner, W.; Chen, X.; Chen, C. L.; Jiang, J. C.; Meletis, E. I.; Bhalla, A. *Appl. Phys. Lett.* **2004**, *85*, 3202–3204.
(6) Lin, Y.; Chen, X.; Liu, S. W.; Chen, C. L.; Lee, J. S.; Li, Y.; Jia, Q. X.; Bhalla, A. *Appl. Phys. Lett.* **2004**, *84*, 577–579.
(7) Jiang, J. C.; Lin, Y.; Chen, C. L.; Chu, C. W.; Meletis, E. I. *J. Appl. Phys.* **2002**, *91*, 3188–3192.
(8) Chen, C. L.; Shen, J.; Chen, S. Y.; Luo, G. P.; Chu, C. W.; Miranda, F. A.; Van Keuls, F. W.; Jiang, J. C.; Meletis, E. I.; Chang, H. Y. *Appl. Phys. Lett.* **2001**, *78*, 652–654.
(9) Huang, D. X.; Chen, C. L.; Jacobson, A. J. *J. Appl. Phys.* **2005**, *97*, 043506.
(10) Lin, X.; He, X. B.; Yang, T. Z.; Guo, W.; Shi, D. X.; Gao, H. J.; Ma, D. D. D.; Lee, S. T.; Liu, F.; Xie, X. C. *Appl. Phys. Lett.* **2006**, *89*, 043103.
(11) Lin, X.; He, X. B.; Lu, J. L.; Gao, L.; Huan, Q.; Shi, D. X.; Gao, H. J. *Chin. Phys.* **2005**, *14*, 1536–1543.
(12) Kanagawa, T.; Hobara, R.; Matsuda, I.; Tanikawa, T.; Natori, A.; Hasegawa, S. *Phys. Rev. Lett.* **2003**, *91*, 036805.
(13) Wasscher, J. D. *Philips Res. Rep.* **1961**, *16*, 301–306.
(14) Salamon, M. B.; Jaime, M. *Rev. Mod. Phys.* **2001**, *73*, 583–628.
(15) Xiong, Y. M.; Chen, T.; Wang, G. Y.; Chen, X. H.; Chen, X.; Chen, C. L. *Phys. Rev. B* **2004**, *70*, 094407.
(16) Campillo, G.; Berger, A.; Osorio, J.; Pearson, J. E.; Bader, S. D.; Baca, E.; Prieto, P. *J. Magn. Magn. Mater.* **2001**, *237*, 61–68.
(17) Seiro, S.; Koller, E.; Fasano, Y.; Fischer, Ø. *Appl. Phys. Lett.* **2007**, *91*, 091913.
(18) Biswas, A.; Rajeswari, M.; Srivastava, R. C.; Venkatesan, T.; Greene, R. L.; Lu, Q.; de Lozanne, A. L.; Millis, A. J. *Phys. Rev. B* **2001**, *63*, 184424.
(19) Hasegawa, S.; Shiraki, I.; Tanabe, F.; Hobara, R.; Kanagawa, T.; Tanikawa, T.; Matsuda, I.; Petersen, C. L.; Hansen, T. M.; Boggild, P.; Grey., F. *Surf. Rev. Lett.* **2003**, *10*, 963–980.

AM100542N